# Distributed Stochastic Scheduling of Massive Backup Batteries in Cellular Networks for Operational Reserve and Frequency Support Ancillary Services

Kun Li, *Student Member*, *IEEE*, Jiakun Fang, *Senior Member*, *IEEE*, Xiaomeng Ai, *Member*, *IEEE*, Shichang Cui, *Member*, *IEEE*, Rongkang Zhao, *Student Member*, *IEEE*, and Jinyu Wen, *Member*, *IEEE*

***Abstract*—Base station (BS) backup batteries (BSBBs), with their dispatchable capacity, are potential demand-side resources for future power systems. To enhance the power supply reliability and post-contingency frequency security of power systems, we propose a two-stage stochastic unit commitment (UC) model incorporating operational reserve and post-contingency frequency support provisions from massive BSBBs in cellular networks, in which the minimum backup energy demand is considered to ensure BS power supply reliability. The energy, operational reserve, and frequency support ancillary services are co-optimized to handle the power balance and post-contingency frequency security in both forecasted and stochastic variable renewable energy (VRE) scenarios. Furthermore, we propose a dedicated and scalable distributed optimization framework to enable autonomous optimizations for both dispatching center (DC) and BSBBs. The BS model parameters are stored and processed locally, while only the values of BS decision variables are required to upload to DC under the proposed distributed optimization framework, which safeguards BS privacy effectively. Case studies on a modified IEEE 14-bus system demonstrate the effectiveness of the proposed method in promoting VRE accommodation, ensuring post-contingency frequency security, enhancing operational economics, and fully utilizing BSBBs' energy and power capacity. Besides, the proposed distributed optimization framework has been validated to converge to a feasible solution with near-optimal performance within limited iterations. Additionally, numerical results on the Guangdong 500 kV provincial power system in China verify the scalability and practicality of the proposed distributed optimization framework.**

***Index Terms*—Base station, backup battery, operational reserve, frequency security, distributed optimization, privacy.**

## NOMENCLATURE

### A. Indices

| | |
|---|---|
| $i, j, k, l, m$ | Synchronous generator (SG), variable renewable energy (VRE), base station (BS) or BS backup battery (BSBB), load, and SG segment indices |
| $n$ | Iteration index |
| $s$ | Stochastic scenario index |
| $t$ | Period index |

### B. Parameters

| | |
|---|---|
| $\alpha_k^{BS}, \beta_k^{BS}$ | Coefficients of power consumption model of BS $k$ |
| $\Delta P^0$ | Power disturbance |
| $\Delta t$ | Duration of a single period (1 hour) |
| $\lambda_{k,n}^{BSBB}$ | Dual variables corresponding to auxiliary constraints of BS $k$ |
| $\varepsilon_1, \varepsilon_2$ | Given parameters for convergence criteria |
| $\pi_s$ | Probability of stochastic scenario $s$ |
| $c_i^{G,re}, c_k^{BSBB,re}$ | Operational reserve capacity cost coefficients of SG $i$ and BSBB $k$ |
| $c_i^{G,PFR}, c_k^{BSBB,PFR}$ | Primary frequency response (PFR) reserve capacity cost coefficients of SG $i$ and BSBB $k$ |
| $c_k^{BSBB,IR}$ | Inertia response (IR) reserve capacity cost coefficient of BSBB $k$ |
| $c_i^{G,de}, c_k^{BSBB,de}$ | Reserve deployment cost coefficients of SG $i$ and BSBB $k$ |
| $c_k^{BSBB}$ | Charging and discharging cost coefficient of BSBB $k$ |
| $\underline{E_k^{BSBB}}, \overline{E_k^{BSBB}}$ | The minimum and maximum backup energy demands of BSBB $k$ |
| $H_i^G$ | SG $i$ inertia |
| $H^{sys}$ | System inertia |
| $\underline{H^{sys}}$ | Lower bound of system inertia |
| $\overline{K_k^{BSBB}}$ | The maximum droop factor of BSBB $k$ |

Manuscript received: June 16, 2023; revised: August 16, 2023; accepted: September 6, 2023. Date of CrossCheck: September 6, 2023. Date of online publication: November 1, 2023.

This work was supported in part by the National Nature Science Foundation of China (No. 52177088).

This article is distributed under the terms of the Creative Commons Attribution 4.0 International License (http://creativecommons.org/licenses/by/4.0/).

K. Li, J. Fang, X. Ai (corresponding author), S. Cui, R. Zhao, and J. Wen are with State Key Laboratory of Advanced Electromagnetic Engineering and Technology, School of Electrical and Electronic Engineering, Huazhong University of Science and Technology, Wuhan 430074, China (e-mail: likun_20@hust.edu.cn; jfa@hust.edu.cn; xiaomengai@hust.edu.cn; shichang_cui@hust.edu.cn; rongkang_zhao@hust.edu; jinyu.wen@hust.edu.cn).

DOI: 10.35833/MPCE.2023.000414

$K^D$ Load damping coefficient
$K_i^G$ Droop factor of SG $i$
$L_k^{BS}, T_k^{BS}$ Power and traffic loads of BS $k$
$M$ A sufficiently large positive real number
$\overline{P_k^{BS,S}}$ Power source capacity of BS $k$
$\overline{P_k^{BSBB,ch}}$, $\overline{P_k^{BSBB,dis}}$ The maximum charging and discharging power of BSBB $k$
$\overline{P_{i,m}^G}$ The maximum generation of power segment $m$ of SG
$\underline{P_i^G}, \overline{P_i^G}$ The minimum and maximum generation of SG $i$
$\overline{P_i^{G,ru}}, \overline{P_i^{G,rd}}$ Upward and downward ramping capacities of SG $i$
$\overline{f^{RoCoF}}, \overline{\Delta f}, \overline{\Delta f^{ss}}$ Rate of change of frequency (RoCoF), frequency nadir, and quasi-steady-state (QSS) frequency threshold
$\overline{P_j^V}$ The maximum generation of VRE $j$
$T$ Number of periods during the entire schedule horizon
$Tb_k^{BS}$ The minimum backup duration of BS $k$
$T_i^G$ Response constant of SG $i$

### C. Variables

$\delta_j^V$ Curtailment rate of VRE $j$
$\Delta P_k^{BSBB,IR}$ IR reserve deployment of BSBB $k$
$\Delta P_k^{BSBB,nad}$, $\Delta P_k^{BSBB,ss}$ PFR reserve deployment of BSBB $k$ for frequency nadir and QSS frequency support
$\Delta P_i^{G,nad}, \Delta P_i^{G,ss}$ PFR reserve deployment of SG $i$ for frequency nadir and QSS frequency support
$\boldsymbol{A}_k^{BSBB,coup}$ Auxiliary variables for DC for decoupling direct coupling relationships among BSBBs
$\boldsymbol{C}^{DC}$, $\boldsymbol{C}_k^{BS}$ Cost coefficient vectors
$C_i^{G,p}, C_i^{G,su}, C_i^{G,sd}$ Fuel, startup, and shutdown costs of SG $i$
$E_k^{BSBB}$ State of charge (SOC) of BSBB $k$
$H_k^{BSBB}$ Virtual inertia of BSBB $k$
$K_k^{BSBB}$ Droop factor of BSBB $k$
$M$ A sufficiently large positive real number
$P_k^{BSBB}$ Power of BSBB $k$
$P_{k,t}^{BSBB,L}$ Absolute value of $P_k^{BSBB}$
$P_i^G$ Generation of SG $i$
$P_{i,m}^G$ Generation of power segment $m$ of SG $i$
$\overline{R_k^{BSBB,u}}, \overline{R_k^{BSBB,d}}$ Upward and downward operational reserve capacities of BSBB $k$
$\overline{R_k^{BSBB,IR}}$, $\overline{R_k^{BSBB,PFR}}$ IR and primary frequency response (PFR) reserve capacities of BSBB $k$
$R_k^{BSBB,u}, R_k^{BSBB,d}$ Upward and downward reserve deployments of BSBB $k$
$\overline{R_i^{G,PFR}}$ PFR reserve capacity of SG $i$
$\overline{R_i^{G,u}}, \overline{R_i^{G,d}}$ Upward and downward operational reserve capacities of SG $i$
$R_i^{G,u}, R_i^{G,d}$ Upward and downward reserve deployments of SG $i$
$\boldsymbol{r}_{n+1}$ Primal residual in ADMM algorithm
$\boldsymbol{s}_{n+1}$ Dual residual in ADMM algorithm
$\boldsymbol{S}^{sys}$ Feasible region of variables ($\boldsymbol{X}^{DC}$, $\boldsymbol{X}_k^{BSBB,coup}$)
$\boldsymbol{S}_k^{BSBB}$ Vector of decision variables ($\boldsymbol{X}_k^{BSBB,only}$, $\boldsymbol{X}_k^{BSBB,coup}$)
$\boldsymbol{X}_k^{BSBB,only}$, $\boldsymbol{X}_k^{BSBB,coup}$ Vectors of all variables for BSBB $k$

## I. Introduction

THE transition towards net-zero carbon emission has created a shortage of flexibility resources for maintaining power balance in power systems [1], [2]. Simultaneously, the large-scale replacement of synchronous generators (SGs) with inverter-based variable renewable energy (VRE) will result in an increasingly prominent frequency security issue [3], [4]. The scarcity of operational reserve and post-contingency frequency response (including inertial response (IR) and primary frequency response (PFR)) resources will pose a threat to the power system reliability and security [5]. To address these problems, demand-side resources have emerged as potential participants in the provision of ancillary services for the power system, driven by the development of end-user electrification [6]. Among them, the demand response (DR) potential of base station (BS) backup batteries (BSBBs) is increasingly gaining attention.

The fast development of information and communication technology (ICT) has led to a significant increase in the number of constructed 5G BSs. According to the Guangdong Provincial Department of Industry and Information Technology in China, the cumulative number of 5G macro BSs in the province is expected to reach 160000 by 2025 [7], with a total BSBB capacity of 1600 MW, accounting for approximately 1% of the forecasted peak load in Guangdong, China, in 2025 [8]. These massive BSBBs represent a potential resource to provide operational reserve [9] and frequency support services [10] to power systems. However, the primary function of BSBBs currently is to ensure BS power supply reliability, and they have not yet been involved in power system operations. Considering the tidal effect of BS traffic load and the traffic sensitivity of BS power load [8], the demand for BSBB backup energy varies at different times of the day. This renders BSBBs with dispatchable capacity, enabling them to provide operational reserve services to the power system while ensuring the BS power supply reliability. Additionally, the inverter-based BSBBs exhibit fast response capabilities [11], allowing them to provide IR and PFR services to the power system with their spare power capacity, thereby ensuring post-contingency frequency security [12]. Under the current operation mode of cellular networks, the dispatchable energy capacity of BSBBs for power system operations is not utilized, resulting in prolonged periods of idleness and wastage of resources.

Some studies have explored the involvement of BSBBs in power system operation. The dispatchable capacity of BSBBs has been evaluated and utilized for energy services

in [8], [13]. Reference [14] further investigates the potential of the spare capacity of BSBB in stabilizing the photovoltaic (PV) output in 5G BS microgrids. Besides, a rule-based mechanism is constructed to coordinate the spare capacity of massive distributed BSBB to provide secondary frequency regulation service [15]. Reference [16] considers 5G BSBBs as a new flexible resource and uses them to optimize the voltage profile of active distribution networks. Yet few studies have explored the utilization of dispatchable capacity of BSBB for providing operational reserve and frequency support ancillary services, which are of significant value for maintaining the power supply reliability and security in future power systems. And the corresponding model for utilizing BSBBs to provide these ancillary services has not been well-developed, representing a research gap in this field.

Another important aspect to consider is the excessive computational burden brought by centralized optimization when a large number of BSBBs are involved in power system operations. BSBBs are characterized by small individual capacities and a large quantity, and it is impractical to model and optimize the scheduling of such a great number of BSBBs and sizable generation units together in a centralized manner. The aggregation and scheduling of a massive amount of demand-side resources have been extensively studied. The aggregation control of smart buildings for primary frequency support is studied in [17]. The aggregated heating, ventilation, and air conditioning (HVAC) systems are used for ancillary services such as secondary frequency regulation [18], peak shaving [19], and operational reserve [20]. Similarly, electric vehicles are aggregated to smooth the load profile [21], provide frequency control services [22], accommodate VRE generation [23] and handle the VRE uncertainty [24]. Nevertheless, dispatching center (DC) and mobile operators are separate entities, and uploading BSBB model parameters to DC or aggregators poses an inherent risk of privacy breaches, particularly in relation to the BS traffic load profiles [25].

Distributed optimization offers a solution to address both the computational burden brought by massive BSBBs and the need to protect the privacy information of BS. Existing research works have applied distributed optimization to the scheduling of various entities, including microgrids [26], energy communities [27], [28], and electric vehicles [29], aiming to address the computational burden associated with centralized solutions. Besides, some studies have employed distributed optimization to address privacy concerns. The peer-to-peer energy sharing among energy buildings through distributed transactions is studied [30]. Reference [31] proposes a finite-time consensus-based distributed optimization algorithm to solve the economic dispatch problem. A distributed deep reinforcement learning method is proposed for intelligent load scheduling in residential smart grids in [32]. Similar to the above studies, the computational burden and privacy concerns associated with large-scale BSBB scheduling are expected to be addressed through distributed optimization. Nevertheless, the detailed design of the distributed optimization framework dedicated to the scheduling of massive BSBBs has not been well-studied.

Based on the review of the existing research works, two main issues arise when incorporating BSBBs into power system operation: ① developing a model for operational reserve and frequency support provisions for BSBBs, and ② designing a dedicated and scalable distributed optimization framework suitable for the participation of large-scale BSBBs in the cellular networks to address the computational burden and privacy concerns related to the centralized optimization. To fill in the above-mentioned research gaps, this paper proposes a two-stage stochastic unit commitment (UC) model with operational reserve and frequency support provisions from massive BSBBs, in which the dispatchable capacity of each BSBB is evaluated according to the BS traffic load profile. We reformulate the proposed two-stage stochastic UC model to enable distributed optimization, thereby ensuring scalability and protecting the privacy information of BS. Specifically, our main contributions are summarized as follows.

1) To cope with the uncertainty of VRE generation and complement the frequency support resources, we incorporate BSBBs into the operational reserve, IR, and PFR ancillary services, thereby enhancing the reliability and security of future power systems. The corresponding ancillary service provision model for BSBBs is developed considering their minimum backup energy demand to ensure BS power supply reliability.

2) We propose a two-stage stochastic UC model incorporating operational reserve and frequency support provisions from massive BSBBs, in which the energy, operational reserve, IR, and PFR reserve are co-optimized to ensure the power balance and post-contingency frequency security in both forecasted and all stochastic VRE scenarios.

3) A dedicated distributed optimization framework suitable for massive BSBBs is designed and realized through a specific problem reformulation method and the application of the alternating direction method of multiplier (ADMM) algorithm. Notably, our proposed framework enables autonomous optimizations for both DC and individual BS, and all of the BSBB model parameters are stored and processed locally, thereby ensuring its scalability and protecting the privacy security of BS effectively.

The remainder of the paper is organized as follows. Section II develops the two-stage stochastic UC model incorporating operational reserve and frequency support provisions from massive BSBBs. The distributed optimization framework is proposed in Section III. Case studies are conducted in Section IV, and Section V draws the conclusions.

## II. Two-stage Stochastic UC Model Incorporating Operational Reserve and Frequency Support Provisions from Massive BSBBs

In this section, we first evaluate the dispatchable capacity of each BSBB according to its traffic load profile and backup duration demand. Then, the operational reserve and frequency support provision model for BSBBs is proposed, followed by the two-stage stochastic UC model incorporating ancillary services from BSBBs. Finally, the proposed model is linearized.

### A. Evaluating Dispatchable Capacity of BSBBs

Due to the uneven temporal distribution of cellular network businesses, the traffic load $T_{k,t}^{BS}$ of BSs exhibits significant tidal effects [33]. Besides, the power consumption of 5G BSs is traffic-sensitive, which can be modeled as [8]:

$$L_{k,t}^{BS}=\alpha_k^{BS}T_{k,t}^{BS}+\beta_k^{BS} \tag{1}$$

Due to the variation in power consumption of 5G BSs throughout the day, the backup energy demand of BSBBs varies during different time periods, as shown in Fig. 1. This indicates that the backup energy of BSBBs does not need to be constantly at its maximum level, providing potential for their participation in ancillary services for power systems.

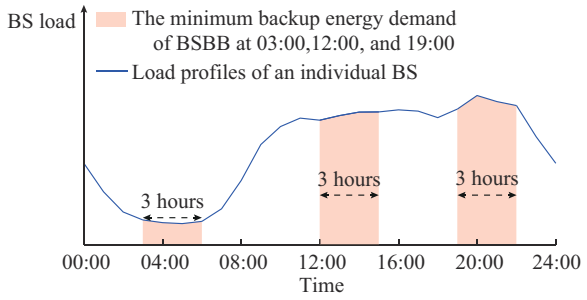


Fig. 1. Evaluation of backup energy demand of BSBBs.

Typically, most of 5G BSs are constructed with BSBBs for a backup duration of 3 hours to meet the reliability requirements for power supply [15]. Thus, the minimum backup energy demand of BSBB $k$ at time instant $t$ can be calculated:

$$\underline{E_{k,t}^{BSBB}}=\int_t^{t+Tb_k^{BS}}L_{k,\tau}^{BS}\mathrm{d}\tau \tag{2}$$

### B. Operational Reserve and Frequency Support Ancillary Service Provision Model for BSBBs

The upward and downward operational reserve capacities and PFR and IR reserve capacities provided by BSBB $k$ should satisfy the following constraints. Without loss of generality, this paper only considers the frequency drop event caused by sudden power shortage.

$$-\overline{P_k^{BSBB,dis}}\le P_{k,t}^{BSBB}\le\overline{P_k^{BSBB,ch}} \tag{3}$$

$$E_{k,t}^{BSBB}=E_{k,t-1}^{BSBB}+P_{k,t}^{BSBB}\Delta t\quad\forall t\ge 1 \tag{4}$$

$$E_{k,T}^{BSBB}=E_{k,0}^{BSBB} \tag{5}$$

$$\underline{E_{k,t}^{BSBB}}\le E_{k,t}^{BSBB}\le\overline{E_k^{BSBB}} \tag{6}$$

$$\begin{cases}\overline{R_{k,t}^{BSBB,u}}\ge 0\\ \overline{R_{k,t}^{BSBB,d}}\ge 0\\ \overline{R_{k,t}^{BSBB,PFR}}\ge 0\\ \overline{R_{k,t}^{BSBB,IR}}\ge 0\\ P_{k,t}^{BSBB}+\overline{R_{k,t}^{BSBB,d}}\le\overline{P_k^{BSBB,ch}}\\ P_{k,t}^{BSBB}-\overline{R_{k,t}^{BSBB,u}}-\overline{R_{k,t}^{BSBB,PFR}}-\overline{R_{k,t}^{BSBB,IR}}\ge-\overline{P_k^{BSBB,dis}}\end{cases} \tag{7}$$

$$P_{k,t}^{BSBB}+\overline{R_{k,t}^{BSBB,d}}+L_{k,t}^{BS}\le\overline{P_k^{BSBB,S}} \tag{8}$$

Formula (3) limits the charging and discharging power of BSBB $k$. Formulas (4)-(6) limit the SoC of BSBB $k$. Formula (7) ensures the sum of operational reserve and PFR/IR reserve capacities is within the power capacity of BSBB. Formula (8) corresponds to the limit of power source capacity of BS.

Utilizing the dispatchable capacity of BSBBs, the upward and downward reserve deployments of BSBB $k$ in stochastic VRE scenario $s$ are expressed as:

$$\begin{cases}R_{s,k,t}^{BSBB,u}\ge 0\\ R_{s,k,t}^{BSBB,d}\ge 0\\ R_{s,k,t}^{BSBB,u}-R_{s,k,t}^{BSBB,d}=P_{k,t}^{BSBB}-P_{s,k,t}^{BSBB}\end{cases} \tag{9}$$

The upward and downward reserve deployments of BSBB $k$ should not exceed their corresponding reserve capacities.

$$\begin{cases}0\le R_{s,k,t}^{BSBB,u}\le\overline{R_{k,t}^{BSBB,u}}\\ 0\le R_{s,k,t}^{BSBB,d}\le\overline{R_{k,t}^{BSBB,d}}\end{cases} \tag{10}$$

Besides, the energy storage of BSBB $k$ in each stochastic scenario $s$ should be subjected to the following constraints.

$$\begin{cases}E_{s,k,t}^{BSBB}=E_{s,k,t-1}^{BSBB}+P_{s,k,t}^{BSBB}\Delta t\quad\forall t\ge 1\\ E_{s,k,T}^{BSBB}=E_{s,k,0}^{BSBB}\\ \underline{E_{k,t}^{BSBB}}\le E_{s,k,t}^{BSBB}\le\overline{E_k^{BSBB}}\end{cases} \tag{11}$$

In addition, the IR/PFR reserve deployment of BSBB $k$ in both the forecasted scenario and stochastic scenario $s$ should not exceed its corresponding operational reserve capacity, respectively.

$$\begin{cases}0\le\Delta P_{k,t}^{BSBB,IR}\le\overline{R_{k,t}^{BSBB,IR}}\\ 0\le\Delta P_{k,t}^{BSBB,nad}\le\overline{R_{k,t}^{BSBB,PFR}}\\ 0\le\Delta P_{k,t}^{BSBB,ss}\le\overline{R_{k,t}^{BSBB,PFR}}\end{cases} \tag{12}$$

$$\begin{cases}0\le\Delta P_{s,k,t}^{BSBB,IR}\le\overline{R_{k,t}^{BSBB,IR}}\\ 0\le\Delta P_{s,k,t}^{BSBB,nad}\le\overline{R_{k,t}^{BSBB,PFR}}\\ 0\le\Delta P_{s,k,t}^{BSBB,ss}\le\overline{R_{k,t}^{BSBB,PFR}}\end{cases} \tag{13}$$

### C. Two-stage Stochastic UC Incorporating Operational Reserve and Frequency Support Ancillary Services for BSBBs

A two-stage optimization problem is proposed to cope with the VRE uncertainties. The first-stage decisions are made in the day-ahead scheduling when the forecasted VRE scenario has been given, including UC, power generation, operational reserve capacity, and frequency support reserve capacity of both SGs and BSBBs. The real-time regulations are made in the second stage to deal with the VRE uncertainties during the intra-day operation process, including the deployment of operational reserve and PFR/IR reserve.

The objective function of the two-stage stochastic UC model is shown as follows:

$$\min\Bigg[\sum_t\sum_i\left(C_{i,t}^{G,p}+C_{i,t}^{G,su}+C_{i,t}^{G,sd}\right)+\sum_t\sum_k c_k^{BSBB}\left|P_{k,t}^{BSBB}\right|+\sum_t\sum_i\left(c_i^{G,re}\overline{R_{i,t}^{G,u}}+c_i^{G,re}\overline{R_{i,t}^{G,d}}\right)+\sum_t\sum_k\left(c_k^{BSBB,re}\overline{R_{k,t}^{BSBB,u}}+c_k^{BSBB,re}\overline{R_{k,t}^{BSBB,d}}\right)+\sum_t\sum_i c_i^{G,PFR}\overline{R_{i,t}^{G,PFR}}+\sum_t\sum_k\left(c_k^{BSBB,PFR}\overline{R_{k,t}^{BSBB,PFR}}+c_k^{BSBB,IR}\overline{R_{k,t}^{BSBB,IR}}\right)+\sum_t\sum_s\pi_s\sum_j\delta_{s,j,t}^{V}\overline{P_{s,j,t}^{V}}+\sum_t\sum_s\pi_s\sum_i\left(c_i^{G,de}R_{s,i,t}^{G,u}+c_i^{G,de}R_{s,i,t}^{G,d}\right)+\sum_t\sum_s\pi_s\sum_k\left(c_k^{BSBB,de}R_{s,k,t}^{BSBB,u}+c_k^{BSBB,de}R_{s,k,t}^{BSBB,d}\right)\Bigg] \tag{14}$$

where the first six terms represent the first-stage operational costs, including the energy costs of SGs, i. e., fuel, startup, and shutdown costs (the first term), energy costs of BSBBs (the second term), the operational reserve capacity costs of SGs (the third term) and BSBBs (the fourth term), the PFR reserve capacity costs of SGs (the fifth term), and the PFR/IR reserve capacity costs of BSBBs (the sixth term), respectively. The second-stage operational costs consist of the penalty for VRE curtailment (the seventh term), operational reserve deployment costs of SGs (the eighth term) and BSBBs (the last term) in the stochastic scenarios.

The first-stage constraints include:

$$\sum_i P_{i,t}^{G}+\sum_j\overline{P_{j,t}^{V}}=\sum_l L_{l,t}+\sum_k P_{k,t}^{BSBB} \tag{15}$$

$$\begin{cases}P_{i,t}^{G}=\underline{P_i^{G}}U_{i,t}^{G}+\sum_m P_{i,m,t}^{G}\\ \underline{P_i^{G}}U_{i,t}^{G}\le P_{i,t}^{G}\le\overline{P_i^{G}}U_{i,t}^{G}\\ 0\le P_{i,m,t}^{G}\le\overline{P_{i,m}^{G}}\end{cases} \tag{16}$$

$$\begin{cases}0\le\overline{R_{i,t}^{G,u}}\le\min\left\{\overline{P_i^{G,ru}}U_{i,t}^{G},\overline{P_{i,t}^{G}}U_{i,t}^{G}-P_{i,t}^{G}\right\}\\ 0\le\overline{R_{i,t}^{G,d}}\le\min\left\{\overline{P_i^{G,rd}}U_{i,t}^{G},P_{i,t}^{G}-\underline{P_{i,t}^{G}}U_{i,t}^{G}\right\}\end{cases} \tag{17}$$

$$0\le\overline{R_{i,t}^{G,PFR}}\le\overline{P_{i,t}^{G}}U_{i,t}^{G}-P_{i,t}^{G}-\overline{R_{i,t}^{G,u}} \tag{18}$$

$$\begin{cases}0\le\Delta P_{i,t}^{G,nad}\le\overline{R_{i,t}^{G,PFR}}\\ \Delta P_{i,t}^{G,nad}\le\dfrac{\Delta P_t^0K_i^{G}}{\pi\underline{H_t^{sys}}}\left(-T_i^{G}+\dfrac{\pi\overline{\Delta f}}{\Delta P_t^0}\underline{H_t^{sys}}+T_i^{G}\mathrm{e}^{-\frac{\pi\overline{\Delta f}}{T_i^{G}\Delta P_t^0}\underline{H_t^{sys}}}\right)\end{cases} \tag{19}$$

$$\begin{cases}0\le\Delta P_{i,t}^{G,ss}\le\overline{R_{i,t}^{G,PFR}}\\ \Delta P_{i,t}^{G,ss}\le K_i^{G}\overline{\Delta f^{ss}}\end{cases} \tag{20}$$

$$\begin{cases}\overline{K_k^{BSBB}}\ge K_{k,t}^{BSBB}\ge 0\\ \Delta P_{k,t}^{BSBB,IR}=2H_{k,t}^{BSBB}\overline{f^{RoCoF}}\\ \Delta P_{k,t}^{BSBB,nad}\le K_{k,t}^{BSBB}\overline{\Delta f}\\ \Delta P_{k,t}^{BSBB,ss}\le K_{k,t}^{BSBB}\overline{\Delta f^{ss}}\end{cases} \tag{21}$$

where the lower bound of system inertia $\underline{H_t^{sys}}$ in (19) can be estimated by the rate of change of frequency (RoCoF) threshold, i. e., $\underline{H_t^{sys}}=\Delta P_t^0/\left(2\overline{f^{RoCoF}}\right)$. Formula (15) ensures the power balance in the forecasted VRE scenario. Formula (16) describes the power limits of SG *i*. Formulas (17) and (18) limit the operational reserve capacity and PFR reserve capacity of SG *i*. Formulas (19) and (20) limit the PFR reserve deployment of SG *i* for frequency nadir and QSS frequency support in the forecasted scenario. Similarly, the limits for PFR/IR reserve deployment of BSBB *k* in the forecasted scenario are shown in (21).

Moreover, we introduce the RoCoF constraints, frequency nadir constraints [34], and QSS frequency constraints to ensure post-contingency frequency security in the forecasted VRE scenario as:

$$\Delta P_t^0\le 2\overline{f^{RoCoF}}\sum_i U_{i,t}^{G}H_i^{G}+\Delta P_{k,t}^{BSBB,IR} \tag{22}$$

$$\Delta P_t^0\le\sum_i\Delta P_{i,t}^{G,nad}+\sum_k\Delta P_{k,t}^{BSBB,nad}+K_t^{D}\overline{\Delta f} \tag{23}$$

$$\Delta P_t^0\le\sum_i\Delta P_{i,t}^{G,ss}+\sum_k\Delta P_{k,t}^{BSBB,ss}+K_t^{D}\overline{\Delta f^{ss}} \tag{24}$$

The other first-stage constraints include (3)-(8), (12), energy cost constraints, ramping limit constraints and minimum online/offline time constraints for SGs, and power flow constraints for transmission lines in the forecasted VRE scenario [35].

The second-stage constraints are shown as follows:

$$\sum_i\left(R_{s,i,t}^{G,u}-R_{s,i,t}^{G,d}\right)+\left[\left(1-\delta_{s,j,t}^{V}\right)\overline{P_{s,j,t}^{V}}-\overline{P_{j,t}^{V}}\right]+\sum_k\left(R_{s,k,t}^{BSBB,u}-R_{s,k,t}^{BSBB,d}\right)=0 \tag{25}$$

$$\begin{cases}0\le R_{s,i,t}^{G,u}\le\overline{R_{i,t}^{G,u}}\\ 0\le R_{s,i,t}^{G,d}\le\overline{R_{i,t}^{G,d}}\end{cases} \tag{26}$$

$$0\le\delta_{s,j,t}^{V}\le 1 \tag{27}$$

Formula (25) ensures the power balance in each stochastic scenario *s*. Formula (26) limits the reserve deployment of SG *i*, while (27) limits the curtailment rate of VRE *j*.

Moreover, the constraints related to post-contingency frequency security in stochastic scenarios, i.e., (19)-(24), are also included, with an index *s* added to them. The detailed models are not presented for brevity.

The other second-stage constraints also include (9) - (11), (13), ramping limit constraints for SGs, and power flow constraints for transmission lines in each stochastic VRE scenario *s* [35].

Without loss of generality, the model proposed in this paper does not incorporate the distribution network models. In specific cases such as distribution line congestions, the solutions obtained may lead to physically infeasible outcomes. Nevertheless, the proposed model can be extended to encompass the consideration for distribution networks, thus mitigating the aforementioned issues.

### *D. Model Linearization*

The nonlinear absolute value term $\left|P_{k,t}^{BSBB}\right|$ in the objective function (14) is recast into a linear one by introducing auxiliary variables $\left\{P_{k,t}^{BSBB,L}\right\}$. The auxiliary variables are subjected to:

$$\begin{cases}P_{k,t}^{BSBB,L}\ge P_{k,t}^{BSBB}\\ P_{k,t}^{BSBB,L}\ge -P_{k,t}^{BSBB}\end{cases} \tag{28}$$

## III. Problem Reformulation for Distributed Implementations

The existence of massive BSs makes it challenging for DC to collect detailed BS model parameters and conduct centralized solving. Worse still, BSs are also reluctant to share their information with DC due to privacy and security concerns. In this section, we first equivalently reformulate the original model into a decomposable form. Then, a distributed optimization framework is proposed using the ADMM algorithm to enable autonomous optimization for both DC and BSs. Finally, we highlight the potential for scalable application and privacy protection of the proposed distributed optimization framework.

### A. Problem Reformulation

We categorize the entities involved in the proposed two-stage stochastic UC model into two main components: DC and BSBBs, where DC is responsible for optimizing the scheduling of SGs, VRE stations, and transmission lines, while BSs optimize their own decision variables. Then, the proposed two-stage stochastic UC model can be abstracted into the following form.

$$\begin{cases} \min \left\{ \left(\boldsymbol{C}^{DC}\right)^{\mathrm{T}} \boldsymbol{X}^{DC} + \sum_k \left(\boldsymbol{C}_k^{BSBB}\right)^{\mathrm{T}} \left[ \left(\boldsymbol{X}_k^{BSBB,only}\right)^{\mathrm{T}} \left(\boldsymbol{X}_k^{BSBB,coup}\right)^{\mathrm{T}} \right]^{\mathrm{T}} \right\} \\ \text{s.t.} \ \left(\boldsymbol{X}^{DC}, \boldsymbol{X}_k^{BSBB,coup}\right) \in \boldsymbol{S}^{sys} \\ \quad \left(\boldsymbol{X}_k^{BSBB,only}, \boldsymbol{X}_k^{BSBB,coup}\right) \in \boldsymbol{S}_k^{BSBB} \end{cases} \tag{29}$$

Specifically, $\boldsymbol{X}^{DC}$ includes all variables for SGs, VRE stations, transmission lines, and power system, including but not limited to $\left\{C_i^{G,p}, C_i^{G,su}, C_i^{G,sd}\right\}$, $\left\{U_i^G\right\}$, $\left\{P_i^G, P_{i,m}^G\right\}$, $\left\{\overline{R_i^{G,u}}, \overline{R_i^{G,d}}\right\}$, $\left\{\overline{R_i^{G,FR}}\right\}$, $\left\{R_i^{G,u}, R_i^{G,d}\right\}$, $\left\{\Delta P_i^{G,nad}, \Delta P_i^{G,ss}\right\}$, $\left\{\delta_j^V\right\}$. $\boldsymbol{X}_k^{BSBB,only}$ and $\boldsymbol{X}_k^{BSBB,coup}$ include all variables for BS $k$, where $\boldsymbol{X}_k^{BSBB,only}$ includes variables that only directly related to BS $k$ itself, i. e., $\left\{E_k^{BSBB}\right\}$, $\left\{\overline{R_k^{BSBB,u}}, \overline{R_k^{BSBB,d}}\right\}$, $\left\{\overline{R_k^{BSBB,IR}}, \overline{R_k^{BSBB,PFR}}\right\}$, $\left\{K_k^{BSBB}\right\}$, and $\left\{H_k^{BSBB}\right\}$, and the variables in $\boldsymbol{X}_k^{BSBB,coup}$ are directly coupled with the variables in $\boldsymbol{X}^{DC}$, including $\left\{P_k^{BSBB}, P_k^{BSBB,L}\right\}$, $\left\{P_k^{BSBB,IR}, \Delta P_k^{BSBB,nad}, \Delta P_k^{BSBB,ss}\right\}$, and $\left\{R_k^{BSBB,u}, R_k^{BSBB,d}\right\}$.

The original model (29) is an approximate $N$-block structure optimization problem, as shown in Fig. 2(a), where $\boldsymbol{X}$ denotes all decision variables in the two-stage stochastic UC problem and $\boldsymbol{b}$ denotes the constant terms in the constraints of the two-stage stochastic UC problem. However, some constraints in $\boldsymbol{S}^{sys}$ such as power balance and frequency security constraints directly couple the decision variables of all SGs, hindering the decomposition of (29). Applying a distributed algorithm such as ADMM directly to (29) would result in the inability to decompose the optimizations for massive BSs. Consequently, achieving autonomous optimization of individual BSs would be unattainable, thus failing to effectively address the challenges arising from limited computational resources and privacy concerns associated with the extensive involvement of BSs. To address this, we introduce a set of auxiliary variables $\boldsymbol{A}_k^{BSBB,coup}$ for DC to decouple the direct coupling relationships among BSBBs, as shown in Fig. 2(b) and (30).

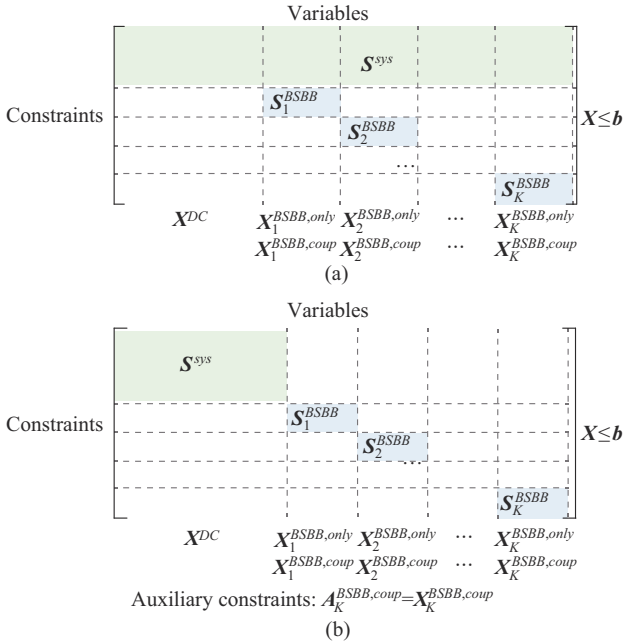


Fig. 2. Problem reformulation of original model. (a) Approximate $N$-block structure optimization. (b) Decoupling direct coupling relationships among BSBBs.

$$\begin{cases} \min \left\{ \left(\boldsymbol{C}^{DC}\right)^{\mathrm{T}} \boldsymbol{X}^{DC} + \sum_k \left(\boldsymbol{C}_k^{BSBB}\right)^{\mathrm{T}} \left[ \left(\boldsymbol{X}_k^{BSBB,only}\right)^{\mathrm{T}} \left(\boldsymbol{X}_k^{BSBB,coup}\right)^{\mathrm{T}} \right]^{\mathrm{T}} + \right. \\ \quad \left. \delta^{sys}\left(\boldsymbol{X}^{DC}, \boldsymbol{A}_k^{BSBB,coup}\right) + \sum_k \delta_k^{BSBB}\left(\boldsymbol{X}_k^{BSBB,only}, \boldsymbol{X}_k^{BSBB,coup}\right) \right\} \\ \text{s.t.} \ \boldsymbol{A}_k^{BSBB,coup} = \boldsymbol{X}_k^{BSBB,coup} \end{cases} \tag{30}$$

where the indicator functions are given:

$$\delta^{sys}\left(\boldsymbol{X}^{DC}, \boldsymbol{X}_k^{BSBB,coup}\right) = \begin{cases} 0 & \left(\boldsymbol{X}^{DC}, \boldsymbol{X}_k^{BSBB,coup}\right) \in \boldsymbol{S}^{sys} \\ M & \left(\boldsymbol{X}^{DC}, \boldsymbol{X}_k^{BSBB,coup}\right) \notin \boldsymbol{S}^{sys} \end{cases} \tag{31}$$

$$\delta_k^{BSBB}\left(\boldsymbol{X}_k^{BSBB,only}, \boldsymbol{X}_k^{BSBB,coup}\right) = \begin{cases} 0 & \left(\boldsymbol{X}_k^{BSBB,only}, \boldsymbol{X}_k^{BSBB,coup}\right) \in \boldsymbol{S}_k^{BSBB} \\ M & \left(\boldsymbol{X}_k^{BSBB,only}, \boldsymbol{X}_k^{BSBB,coup}\right) \notin \boldsymbol{S}_k^{BSBB} \end{cases} \tag{32}$$

### B. Distributed Implementations Using ADMM Algorithm

The augmented Lagrangian function of problem (30) is given as:

$$\begin{aligned} L = & \left(\boldsymbol{C}^{DC}\right)^{\mathrm{T}} \boldsymbol{X}^{DC} + \left(\boldsymbol{C}_k^{BSBB}\right)^{\mathrm{T}} \left( \left(\boldsymbol{X}_k^{BSBB,only}\right)^{\mathrm{T}} \left(\boldsymbol{X}_k^{BSBB,coup}\right)^{\mathrm{T}} \right)^{\mathrm{T}} + \\ & \delta^{sys}\left(\boldsymbol{X}^{DC}, \boldsymbol{A}_k^{BSBB,coup}\right) + \sum_k \delta_k^{BSBB}\left(\boldsymbol{X}_k^{BSBB,only}, \boldsymbol{X}_k^{BSBB,coup}\right) + \\ & \sum_k \left(\boldsymbol{\lambda}_k^{BSBB}\right)^{\mathrm{T}} \left(\boldsymbol{A}_k^{BSBB,coup} - \boldsymbol{X}_k^{BSBB,coup}\right) + \\ & \frac{\rho}{2} \sum_k \left\| \boldsymbol{A}_k^{BSBB,coup} - \boldsymbol{X}_k^{BSBB,coup} \right\|_2^2 \end{aligned} \tag{33}$$

where $\rho$ is a well-defined given positive parameter. Then, we apply the ADMM algorithm to realize distributed optimization, which is presented in Fig. 3.

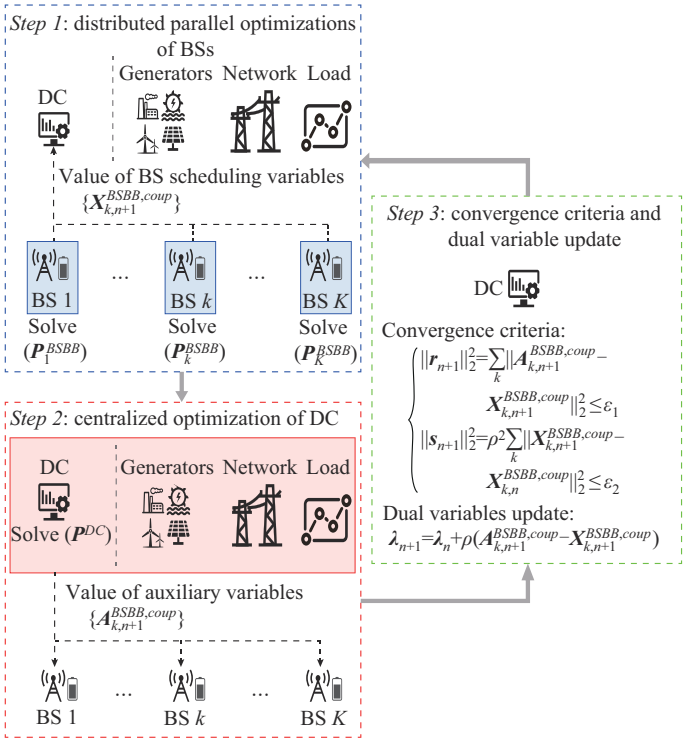


Fig. 3. Distributed optimization framework.

*Step 1*: distributed parallel optimization of BSs. Each BS $k$ parallelly decides its own decision variables $\left(\boldsymbol{X}_{k,n+1}^{BSBB,only}, \boldsymbol{X}_{k,n+1}^{BSBB,coup}\right)$ by solving (33) with the current auxiliary variables $\boldsymbol{A}_{k,n}^{BSBB,coup}$ and dual variables $\boldsymbol{\lambda}_{k,n}^{BSBB}$:

$$\begin{aligned}\min\Big\{&\left(\boldsymbol{C}_k^{BSBB}\right)^{\mathrm{T}}\left[\left(\boldsymbol{X}_k^{BSBB,only}\right)^{\mathrm{T}}\left(\boldsymbol{X}_k^{BSBB,coup}\right)^{\mathrm{T}}\right]^{\mathrm{T}}+\\&\delta_k^{BSBB}\left(\boldsymbol{X}_k^{BSBB,only},\boldsymbol{X}_k^{BSBB,coup}\right)+\left(\boldsymbol{\lambda}_{k,n}^{BSBB}\right)^{\mathrm{T}}\left(\boldsymbol{A}_{k,n}^{BSBB,coup}-\right.\\&\left.\boldsymbol{X}_k^{BSBB,coup}\right)+\frac{\rho}{2}\left\|\boldsymbol{A}_{k,n}^{BSBB,coup}-\boldsymbol{X}_k^{BSBB,coup}\right\|_2^2\end{aligned}\tag{34}$$

Formula (34) is equivalent to the following problem $\left(\boldsymbol{P}_k^{BSBB}\right)$.

$$\begin{cases}\left(\boldsymbol{P}_k^{BSBB}\right):\min\Big\{\left(\boldsymbol{C}_k^{BSBB}\right)^{\mathrm{T}}\left[\left(\boldsymbol{X}_k^{BSBB,only}\right)^{\mathrm{T}}\left(\boldsymbol{X}_k^{BSBB,coup}\right)^{\mathrm{T}}\right]^{\mathrm{T}}+\\\quad\left(\boldsymbol{\lambda}_{k,n}^{BSBB}\right)^{\mathrm{T}}\left(\boldsymbol{A}_{k,n}^{BSBB,coup}-\boldsymbol{X}_k^{BSBB,coup}\right)+\frac{\rho}{2}\left\|\boldsymbol{A}_{k,n}^{BSBB,coup}-\boldsymbol{X}_k^{BSBB,coup}\right\|_2^2\Big\}\\\text{s.t.}\ \left(\boldsymbol{X}_k^{BSBB,only},\boldsymbol{X}_k^{BSBB,coup}\right)\in\boldsymbol{S}_k^{BSBB}\end{cases}\tag{35}$$

Then each BS $k$ will submit its decisions $\boldsymbol{X}_{k,n+1}^{BSBB,coup}$ to DC.

*Step 2*: centralized optimization of DC. DC optimizes the decision variables $\boldsymbol{X}_{n+1}^{DC}$ and auxiliary variables $\boldsymbol{A}_{k,n+1}^{BSBB,coup}$ according to the current decision variables $\boldsymbol{X}_{k,n+1}^{BSBB,coup}$ of each BS $k$ and dual variables $\boldsymbol{\lambda}_{k,n}^{BSBB}$:

$$\begin{aligned}\min\Big[&\left(\boldsymbol{C}^{DC}\right)^{\mathrm{T}}\boldsymbol{X}^{DC}+\delta^{sys}\left(\boldsymbol{X}^{DC},\boldsymbol{A}_k^{BSBB,coup}\right)+\\&\sum_k\left(\boldsymbol{\lambda}_{k,n}^{BSBB}\right)^{\mathrm{T}}\left(\boldsymbol{A}_k^{BSBB,coup}-\boldsymbol{X}_{k,n+1}^{BSBB,coup}\right)+\frac{\rho}{2}\sum_k\left\|\boldsymbol{A}_k^{BSBB,coup}-\boldsymbol{X}_{k,n+1}^{BSBB,coup}\right\|_2^2\Big]\end{aligned}\tag{36}$$

Formula (36) is equivalent to the following problem $\left(\boldsymbol{P}^{DC}\right)$.

$$\begin{cases}\left(\boldsymbol{P}^{DC}\right):\Big[\min\left(\boldsymbol{C}^{DC}\right)^{\mathrm{T}}\boldsymbol{X}^{DC}+\sum_k\left(\boldsymbol{\lambda}_{k,n}^{BSBB}\right)^{\mathrm{T}}\left(\boldsymbol{A}_k^{BSBB,coup}-\boldsymbol{X}_{k,n+1}^{BSBB,coup}\right)+\\\quad\frac{\rho}{2}\sum_k\left\|\boldsymbol{A}_k^{BSBB,coup}-\boldsymbol{X}_{k,n+1}^{BSBB,coup}\right\|_2^2\Big]\\\text{s.t.}\ \left(\boldsymbol{X}^{DC},\boldsymbol{A}_k^{BSBB,coup}\right)\in\boldsymbol{S}^{sys}\end{cases}\tag{37}$$

Then, DC will distribute the auxiliary variable $\boldsymbol{A}_{k,n+1}^{BSBB,coup}$ to each BS $k$.

*Step 3*: update of convergence criteria and dual variables. DC first verifies whether the convergence criteria in (38) are met.

$$\begin{cases}\left\|\boldsymbol{r}_{n+1}\right\|_2^2=\sum_k\left\|\boldsymbol{A}_{k,n+1}^{BSBB,coup}-\boldsymbol{X}_{k,n+1}^{BSBB,coup}\right\|_2^2\le\varepsilon_1\\\left\|\boldsymbol{s}_{n+1}\right\|_2^2=\rho^2\sum_k\left\|\boldsymbol{X}_{k,n+1}^{BSBB,coup}-\boldsymbol{X}_{k,n}^{BSBB,coup}\right\|_2^2\le\varepsilon_2\end{cases}\tag{38}$$

The first criterion is used to determine whether the solution $\boldsymbol{X}_{k,n+1}^{BSBB,coup}$, $\boldsymbol{X}_{k,n+1}^{BSBB,only}$ and $\boldsymbol{X}_{k,n+1}^{BSBB,coup}$ is a feasible one of the original problem, while the second criterion verifies whether the optimal solution has been reached.

If convergence criteria in (38) are satisfied, the iteration stops, and the system will be scheduled accordingly. Otherwise, DC will update the dual variables $\boldsymbol{\lambda}_{k,n+1}^{BSBB}$, as shown in (39), and then send them to the corresponding BS $k$. Subsequently, the process returns to *Step 1*.

$$\boldsymbol{\lambda}_{k,n+1}^{BSBB}=\boldsymbol{\lambda}_{k,n}^{BSBB}+\rho\left(\boldsymbol{A}_{k,n+1}^{BSBB,coup}-\boldsymbol{X}_{k,n+1}^{BSBB,coup}\right)\tag{39}$$

### C. Scalable Applications and Privacy Protection

The proposed distributed optimization framework holds great potential for scalable applications where massive BSs participate in power system operations. In *Step 1*, each BS $k$ solves its own optimization problem $\left(\boldsymbol{P}_k^{BSBB}\right)$ in an autonomous, distributed, and parallel manner. As for *Step 2*, the number of auxiliary variables $\boldsymbol{A}_k^{BSBB,coup}$ in $\left(\boldsymbol{P}^{DC}\right)$ increases linearly with the number of BSs involved. Nevertheless, all auxiliary variables are continuous, and the increase in the number of BSs will not lead to an increase in the number of constraints in $\left(\boldsymbol{P}^{DC}\right)$. Accordingly, the increase of BSs does not significantly amplify the complexity of solving $\left(\boldsymbol{P}^{DC}\right)$. In conclusion, under the proposed distributed optimization framework, the computational burden caused by massive BSs can be shared through distributed computing. Consequently, it is suitable for scalable applications.

Besides, under the proposed distributed optimization framework, the only information that BSs need to submit to DC is the values of their decision variables $\boldsymbol{X}_k^{BSBB,coup}$. In addition, the model parameters of BSBBs, i. e., those in (3)-(13), as well as their traffic load profiles are stored and processed locally, which effectively protect the privacy of cellular networks.

## IV. Case Studies

The effectiveness and scalability of the proposed model are validated on a modified IEEE 14-bus system and Guangdong 500 kV provincial power system in Southern China, re-

spectively. All optimization problems are handled on the MATLAB platform and solved by the commercial solver GUROBI, while all dynamic response process simulations are conducted on MATLAB/Simulink. The simulations are carried out on a computer with an Intel Core i5-10400F@ 2.90 GHz CPU and 24 GB RAM. The optimization gap is set to be $1\times10^{-4}$.

### A. Basic Data of Modified IEEE 14-bus System

The illustrative example is conducted on a modified IEEE 14-bus system, as shown in Fig. 4. There are 5 SGs in the system, whose parameters are shown in Table I. The maximum total load is 362.6 MW. The cost of operational reserve capacity, reserve deployment, and PFR reserve capacity for SGs are set to be 0.4, 1.3, and 1.3 times their highest incremental prices, respectively [20]. The total forecasted wind and load power curves are shown in Fig. 5, and the green shaded area denotes the forecasted error range of wind power. The penalty of wind power curtailment is set to be 200 $/MWh. Five hundred stochastic wind scenarios are generated within 10% forecasted error, and then reduced to 20 representative scenarios by the method in [35].

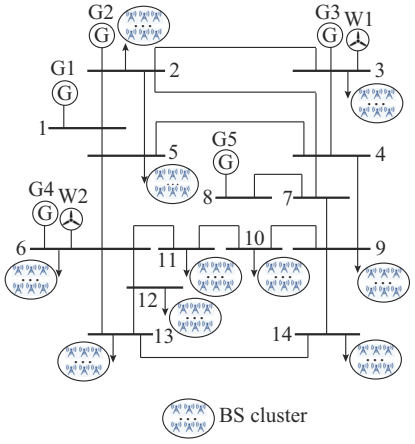


Fig. 4. Modified IEEE 14-bus system.

TABLE I
TECHNICAL PARAMETERS OF SGS IN IEEE 14-BUS SYSTEM

| Unit | Capacity (MW) | The minimum generation (MW) | Ramping capacity (MW/h) | Inertia constant (s) | Droop factor | Response constant (s) |
|---|---|---|---|---|---|---|
| G1 | 332 | 116 | 133 | 4.0 | 35 | 3 |
| G2 | 140 | 49 | 56 | 4.0 | 35 | 3 |
| G3 | 100 | 35 | 40 | 3.5 | 35 | 3 |

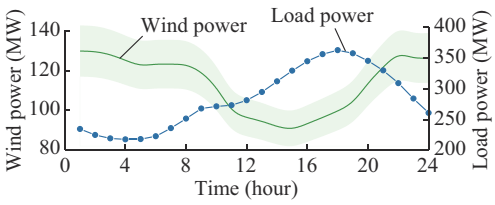


Fig. 5. Forecasted wind and load power curves.

Besides, BSs are supposed to be installed at each load bus, and the total BS capacity is set to be approximately 1% of the peak load at that bus. Thus, 360 BSs are deployed in the system. For each BS, the power source capacity is 12 kW, and the charging/discharging power capacity and energy capacity of each BSBB are set to be 10 kW and 30 kWh, respectively [36]. The BSBB prices for operational reserve capacity, reserve deployment, and PFR/IR reserve capacity are set to be 12 $/MWh, 30 $/MWh, and 30 $/MW, respectively, and the maximum droop factor is set to be 50 [37], [38].

The disturbance $\Delta P_t^0$ is assumed to be 5% of the total load during period $t$. The nominal frequency is set to be 50 Hz, and the threshold of RoCoF, frequency nadir, and QSS frequency are set to be 0.5 Hz/s, 0.5 Hz, and 0.3 Hz, respectively [3].

Three cases are set and compared to verify the effectiveness of the proposed two-stage stochastic UC model.

Case 1: BSBBs with dispatchable capacity are only allowed to provide energy services.

Case 2: BSBBs with dispatchable capacity are allowed to provide energy and operational reserve services.

Case 3: BSBBs with dispatchable capacity are allowed to provide energy, operational reserve, and post-contingency frequency support ancillary services.

### B. Effectiveness Validations of Operational Reserve Capacity and Deployment Demand, and Post-contingency Frequency Security

The operational reserve capacity and deployment demand in all stochastic wind scenarios and post-contingency frequency security metrics in cases 1-3 are shown in Fig. 6 and Fig. 7, respectively.

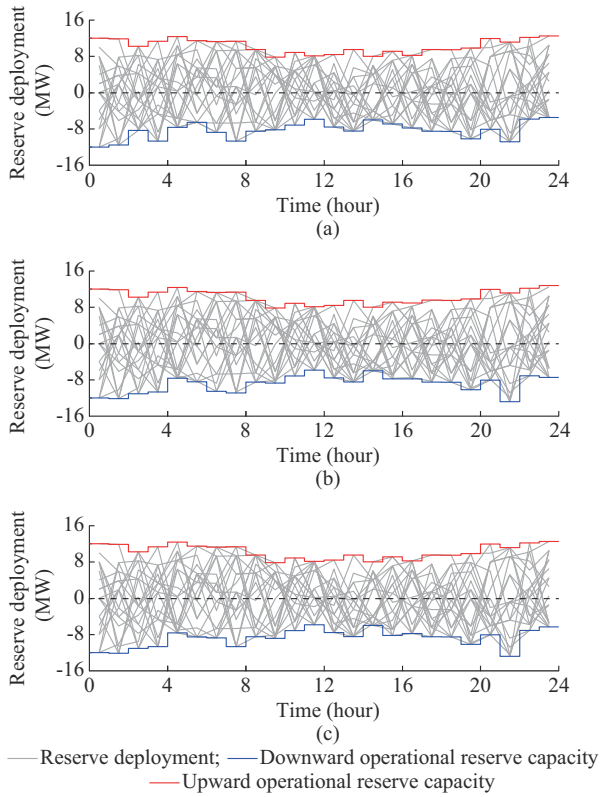


Fig. 6. Operational reserve capacity and deployment demand. (a) Case 1. (b) Case 2. (c) Case 3.

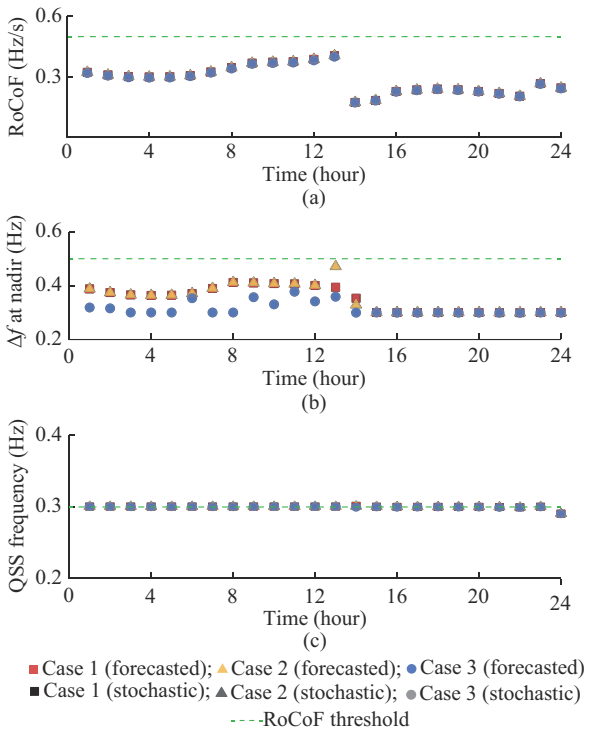


Fig. 7. Post-contingency frequency security metrics. (a) RoCoF. (b) $\Delta f$ at nadir. (c) QSS frequency.

From Fig. 6, it can be observed that the reserve deployment demand in all stochastic wind scenarios can be satisfied by the day-ahead operational reserve capacity, which verifies the effectiveness in maintaining power balance.

Similarly, the simulation results in Fig. 7 show that the RoCoF, frequency nadir, and QSS frequency of cases 1-3 are kept within the corresponding secure thresholds. These verify the effectiveness of the used frequency security constraints.

Moreover, the frequency nadir metric in case 3 is more secure than those in cases 1 and 2, which is attributed to the fast response feature of BSBBs.

It should be mentioned that, as this paper does not account for the uncertainty of disturbances and the IR/PFR reserve capacity is determined in the day-ahead scheduling stage, the post-contingency frequency security metrics in the dynamic simulation results remain the same for both forecasted and stochastic scenarios in the same case.

### *C. Benefits for BSBB Utilizations and Operational Economics*

The detailed operational costs of cases 1-3 are compared in Table II. Besides, the scheduling results of massive BSBBs are shown in Fig. 8, where SoC stands for state of charge.

TABLE II
COMPARISON OF OPERATIONAL COSTS

| Case | Total cost ($) | First-stage start up/ shut down cost ($) | First-stage energy cost ($) | | | First-stage reserve of SG | Capacity cost ($) | | First-stage PFR/IR of SG | Reserve cost ($) | | Second-stage reserve deployment cost ($) | | | Second-stage wind curtailment penalty ($) |
|---|---|---|---|---|---|---|---|---|---|---|---|---|---|---|---|
| | | | SG | BSBB | Total | | BSBB | Total | | BSBB | Total | SG | BSBB | Total | |
| 1 | 184854 | 14310 | 136770 | 198 | 136968 | 7911 | 0 | 7911 | 17301 | 0 | 17301 | 7478 | 0 | 7478 | 885 |
| 2 | 183304 | 14310 | 136872 | 136 | 137008 | 6263 | 1273 | 7536 | 17171 | 0 | 17171 | 5705 | 992 | 6697 | 583 |
| 3 | 181715 | 14310 | 136608 | 131 | 136739 | 7021 | 760 | 7781 | 13264 | 1950 | 15214 | 6399 | 630 | 7029 | 641 |

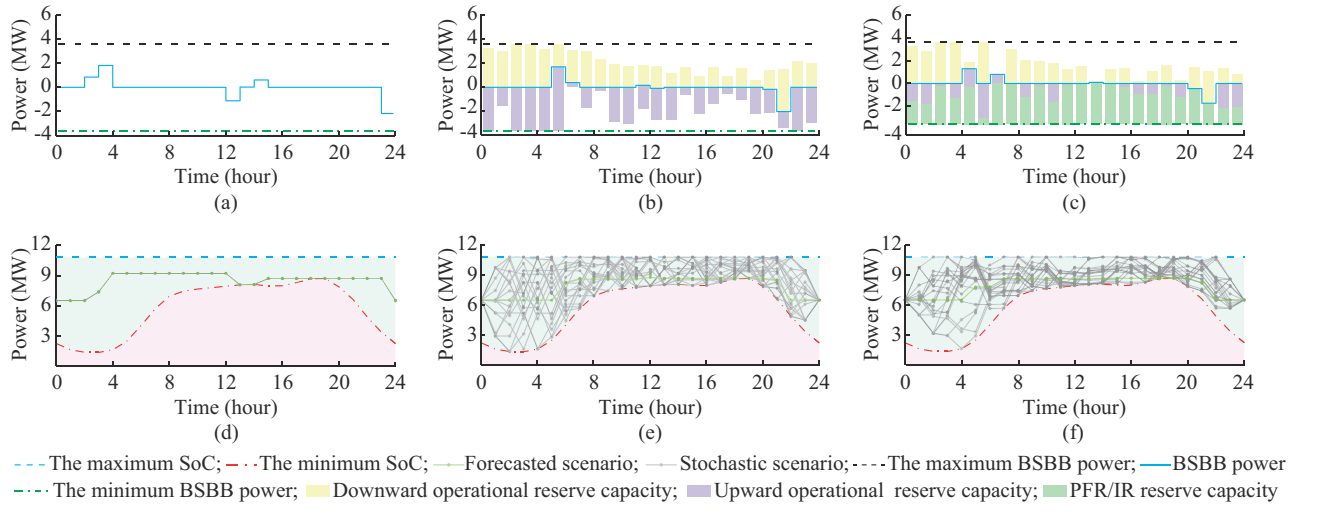


Fig. 8. Scheduling results of massive BSBBs. (a) Case 1 (power and operational reserve capacity of BSBBs). (b) Case 2 (power and operational reserve capacity of BSBBs). (c) Case 3 (power and operational reserve capacity of BSBBs). (d) Case 1 (SoC of BSBBs). (e) Case 2 (SoC of BSBBs). (f) Case 3 (SoC of BSBBs).

In case 1, massive BSBBs are only allowed to provide energy service, and the dispatch result of BSBBs is shown in Fig. 8(a) and (d). The limited utilization of BSBB energy capacity is evident. This can be attributed to the fact that dur-

ing the peak load period (16-20 hours) of the power system, the load demand of BSs also reaches its highest level of the day. Consequently, there is a high demand for backup energy of BSBB, and their dispatchable capacity is small. As a result, the capability of BSBBs in peak shaving is constrained.

Compared with case 1, BSBBs are further allowed to provide operational reserve services in case 2, which reduces the pressure on SGs to ensure power balance. Additionally, it enhances the overall reserve capability of the power system and reduces wind curtailment. The above results have led to a 0.84% improvement in the total operational cost of the power system. From Fig. 8(b) and (e), we can observe that during leisure hours of BS such as 0-6 and 23-24 hours, the power capacity of BSBB can be fully utilized to provide operational reserve services. However, during busy periods of BS, i.e., 8-20 hours, the operational reserve capacity provided by BSBBs is at a relatively low level throughout the day. This is because the dispatchable capacity of BSBBs is limited during those periods, and accordingly, their power capacity is underutilized. Otherwise, it may compromise the security of BSBB operations or impact the reliability of the BS power supply. Therefore, the power capacity utilization of BSBBs is not sufficient during busy periods of BS.

Furthermore, BSBBs are allowed to participate in the frequency support ancillary services in case 3. Due to the short duration of the PFR/IR dynamic process, typically around 30 s, the provision of these frequency support services does not have a significant impact on its storage energy. Consequently, the underutilized power capacity of BSBBs in case 2 can be fully utilized in case 3, releasing more flexibility of BSBBs. This reduces the burden on SGs for providing frequency support ancillary services and improves the economic performance of the power system, specifically, with operational cost reductions of 1.70% and 0.87% compared with those of cases 1 and 2, respectively.

### D. Frequency Security Sensitivity Analysis

A sensitivity analysis is conducted on disturbance ratio, as shown in Fig. 9. It can be observed that the total operational cost of case 3 is always the lowest. This is because both the energy and power capacity of massive BSBBs have been fully utilized.

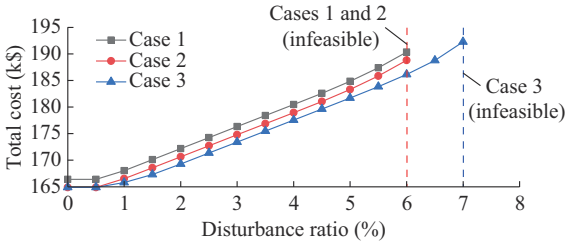


Fig. 9. Sensitivity analysis on disturbance ratio.

Furthermore, compared with cases 1 and 2, case 3 allows BSBBs to provide PFR/IR services, enhancing the system ability to handle sudden power disturbance. Specifically, in cases 1 and 2, the power system can handle a maximum disturbance of approximately 21.8 MW, while in case 3, the ability to handle the maximum power disturbance increases to 25.4 MW.

### E. Convergence Performance of Proposed Distributed Optimization Framework

The iteration process of the proposed distributed optimization framework is presented in Fig. 10. The parameters for the convergence criteria are set as $\varepsilon_1 = 1 \times 10^{-4}$ and $\varepsilon_2 = 1 \times 10^{-4}$, respectively.

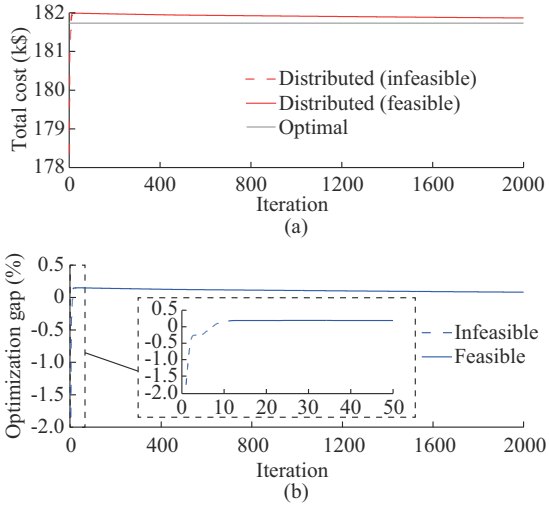


Fig. 10. Convergence performance of proposed distributed optimization framework. (a) Total cost. (b) Optimization gap.

Since the proposed two-stage stochastic UC model is a non-convex optimization problem with integer variables, it is challenging to ensure the convergence to the global optimal solutions when applying the proposed distributed optimization framework. Specifically, the optimization gap converges to 0.08% after 2000 iterations, but does not reach the optimal solution. However, it can also be observed from Fig. 10 that the proposed distributed optimization framework exhibits great convergence performance to a feasible solution. A feasible solution is found after 11 iterations with an acceptable optimization gap of only 0.13%.

The above analysis shows that although the proposed distributed optimization framework cannot guarantee fast convergence to the optimal solution, it is capable of finding a near-optimal feasible solution in a few iterations. In practical applications, DC can balance the trade-off between optimality and computation time to determine when to terminate the iteration process.

### F. Scalability Tests on Guangdong 500 kV Provincial Power System in Southern China

The topology of the Guangdong 500 kV provincial power system in Southern China is shown in Fig. 11, consisting of 280 thermal units (132 coal-fired units and 148 gas-fired units), 20 hydro units, 32 pumped storage stations, 14 nuclear units, 19 PV stations and 32 wind farms with total capacities of 71414 MW, 35431 MW, 1046.5 MW, 9680 MW, 16402 MW, 950 MW, and 12510 MW, respectively. Besides, the system has been interconnected with 14 tie lines, providing a total capacity of 44000 MW to import electric power from other provinces. The maximum total load is set to be 122273 MW, according to the historical data. Moreover, the

planned number of 5G macro BSs to be constructed in Guangdong Province in 2025 is 160000. With such a great number of BSBBs, it is intractable to conduct centralized optimization.

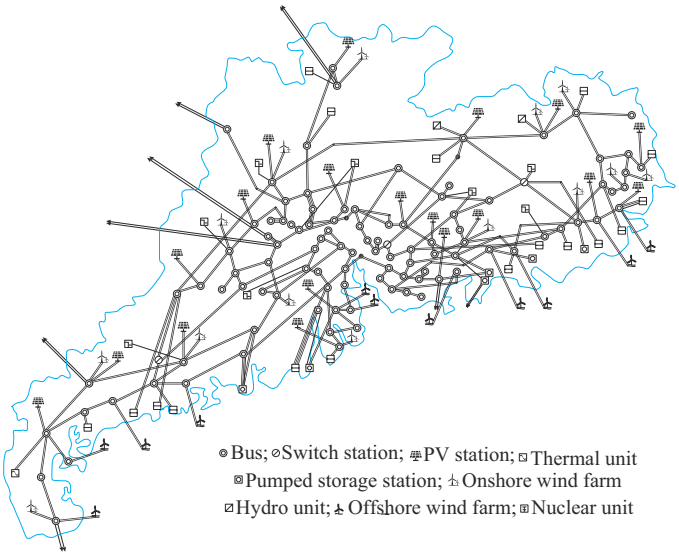


Fig. 11. Topology of Guangdong 500 kV provincial power system in Southern China.

A sensitivity analysis is conducted on the number of BSBBs involved in the ancillary services. We document the number of iterations and corresponding total operational cost when a feasible solution is first found under different numbers of BSs involved, as shown in Fig. 12, where the operational cost without BSBBs is also presented for comparison. We observe that the operational cost decreases as the number of BSBBs involved increases and is always lower than that of the case without BSBB participation. This verifies the effectiveness in enhancing the economics of power system operations.

Besides, the number of iterations required to find a feasible solution does not increase with the number of BSBBs involved. Moreover, the number of iterations (shown as the red dots) is always less than 20. This demonstrates the scalability and practicality of the proposed distributed optimization framework.

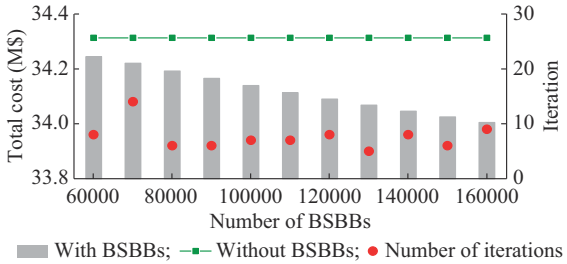


Fig. 12. Sensitivity analysis on number of BSBBs involved in ancillary services.

## V. Conclusion

This paper proposes a two-stage stochastic UC model incorporating operational reserve and post-contingency frequency support ancillary service provisions from massive BSBBs in cellular networks, considering the minimum backup energy demand to ensure the BS power supply reliability. The energy, operational reserve, and frequency support reserve are co-optimized to ensure power balance and frequency security in both forecasted and stochastic VRE scenarios. Furthermore, a distributed optimization framework is proposed to decompose the original problem into two main entities, i.e., DC optimization and BS optimization. The optimization of each BS is autonomous, distributed, and parallel, which ensures great scalability. In addition, both the storage and processing of the BS model parameters are performed locally, and only the values of decision variables are transmitted between the two entities. This effectively protects the privacy of BS data.

Case studies on a modified IEEE 14-bus system demonstrate the effectiveness of the proposed model in promoting VRE accommodation, ensuring post-contingency frequency security, enhancing operational economics, and fully utilizing the dispatchable energy and power capacity of BSBBs. Besides, the proposed distributed optimization framework is validated to converge to a near-optimal feasible solution within a few iterations. Moreover, numerical results on Guangdong 500 kV provincial power system verify the scalability and practicality of the proposed distributed optimization framework.

## References

[1] IEA. (2022, Jan.). World energy outlook 2022. [Online]. Available: https://www.iea.org/reports/world-energy-outlook-2022
[2] S. Impram, S. V. Nese, and B. Oral, "Challenges of renewable energy penetration on power system flexibility: a survey," *Energy Strategy Reviews*, vol. 31, p. 100539, Sept. 2020.
[3] H. Li, Y. Qiao, Z. Lu *et al.,* "Frequency-constrained stochastic planning towards a high renewable target considering frequency response support from wind power," *IEEE Transactions on Power Systems*, vol. 36, no. 5, pp. 4632-4644, Sept. 2021.
[4] J. Li, S. Wang, L. Ye *et al.*, "A coordinated dispatch method with pumped-storage and battery-storage for compensating the variation of wind power," *Protection and Control of Modern Power Systems*, vol. 3, no. 1, p. 2, Mar. 2018.
[5] X. Fu, "Statistical machine learning model for capacitor planning considering uncertainties in photovoltaic power," *Protection and Control of Modern Power Systems*, vol. 7, no. 1, p. 5, Mar. 2022.
[6] A. R. Jordehi, "Optimisation of demand response in electric power systems: a review," *Renewable and Sustainable Energy Reviews*, vol. 103, pp. 308-319, Apr. 2019.
[7] Department of Industry and Information Technology of Guangdong Province. (2020, Jun.). The overall planning of 5G base stations and data centers in Guangdong Province (2021-2025). [Online]. Available: http://gdii.gd.gov.cn/zcgh3227/content/post_3026281.html
[8] P. Yong, N. Zhang, Q. Hou *et al.*, "Evaluating the dispatchable capacity of base station backup batteries in distribution networks," *IEEE Transactions on Smart Grid*, vol. 12, no. 5, pp. 3966-3979, Sept. 2021.
[9] T. P. Teixeira and C. L. T. Borges, "Operation strategies for coordinating battery energy storage with wind power generation and their effects on system reliability," *Journal of Modern Power Systems and Clean Energy*, vol. 9, no. 1, pp. 190-198, Jan. 2021.
[10] U. Datta, A. Kalam, and J. Shi, "Battery energy storage system control for mitigating PV penetration impact on primary frequency control and state-of-charge recovery," *IEEE Transactions on Sustainable Energy*, vol. 11, no. 2, pp. 746-757, Apr. 2020.
[11] Z. Zhang, M. Zhou, Z. Wu *et al.,* "A frequency security constrained scheduling approach considering wind farm providing frequency support and reserve," *IEEE Transactions on Sustainable Energy*, vol. 13, no. 2, pp. 1086-1100, Apr. 2022.
[12] C. Yan, Y. Tang, J. Dai *et al.,* "Uncertainty modeling of wind power

frequency regulation potential considering distributed characteristics of forecast errors," *Protection and Control of Modern Power Systems*, vol. 6, no. 1, p. 22, Mar. 2021.
[13] S. Hu, X. Chen, W. Ni *et al.*, "Modeling and analysis of energy harvesting and smart grid-powered wireless communication networks: a contemporary survey," *IEEE Transactions on Green Communications and Networking*, vol. 4, no. 2, pp. 461-496, Jun. 2020.
[14] X. Ma, Y. Duan, X. Meng *et al.*, "Optimal configuration for photovoltaic storage system capacity in 5G base station microgrids," *Global Energy Interconnection*, vol. 4, no. 5, pp. 465-475, Oct. 2021.
[15] P. Yong, N. Zhang, Y. Liu *et al.*, "Exploring the cellular base station dispatch potential towards power system frequency regulation," *IEEE Transactions on Power Systems*, vol. 37, no. 1, pp. 820-823, Jan. 2022.
[16] Y. Zhou, Q. Wang, Y. Zou *et al.*, "Voltage profile optimization of active distribution networks considering dispatchable capacity of 5G base station backup batteries," *Journal of Modern Power Systems and Clean Energy*, vol. 11, no. 6, pp. 1842-1856, Nov. 2023.
[17] Y. Wang, Y. Xu, and Y. Tang, "Distributed aggregation control of grid-interactive smart buildings for power system frequency support," *Applied Energy*, vol. 251, p. 113371, Oct. 2019.
[18] X. Chen, Q. Hu, Q. Shi *et al.*, "Residential HVAC aggregation based on risk-averse multi-armed bandit learning for secondary frequency regulation," *Journal of Modern Power Systems and Clean Energy*, vol. 8, no. 6, pp. 1160-1167, Nov. 2020.
[19] M. Waseem, Z. Lin, Y. Ding *et al.*, "Technologies and practical implementations of air-conditioner based demand response," *Journal of Modern Power Systems and Clean Energy*, vol. 9, no. 6, pp. 1395-1413, Nov. 2021.
[20] L. Le, J. Fang, X. Ai *et al.,* "Aggregation and scheduling of multi-chiller HVAC systems in continuous-time stochastic unit commitment for flexibility enhancement," *IEEE Transactions on Smart Grid*, vol. 14, no. 4, pp. 2774-2785, Jul. 2023.
[21] C. Wei, J. Xu, S. Liao *et al.*, "Aggregation and scheduling models for electric vehicles in distribution networks considering power fluctuations and load rebound," *IEEE Transactions on Sustainable Energy*, vol. 11, no. 4, pp. 2755-2764, Oct. 2020.
[22] A. Naveed, Ş. Sönmez, and S. Ayasun, "Impact of electric vehicle aggregator with communication time delay on stability regions and stability delay margins in load frequency control system," *Journal of Modern Power Systems and Clean Energy*, vol. 9, no. 3, pp. 595-601, May 2021.
[23] X. Jiang, S. Wang, Q. Zhao *et al.*, "Optimized dispatching method for flexibility improvement of AC-MTDC distribution systems considering aggregated electric vehicles," *Journal of Modern Power Systems and Clean Energy*, vol. 11, no. 6, pp. 1857-1867, Nov. 2023
[24] J. Hu, H. Zhou, Y. Li *et al.*, "Multi-time scale energy management strategy of aggregator characterized by photovoltaic generation and electric vehicles," *Journal of Modern Power Systems and Clean Energy*, vol. 8, no. 4, pp. 727-736, Jul. 2020.
[25] R. Khan, P. Kumar, D. N. K. Jayakody *et al.*, "A survey on security and privacy of 5G technologies: potential solutions, recent advancements, and future directions," *IEEE Communications Surveys & Tutorials*, vol. 22, no. 1, pp. 196-248, Feb. 2020.
[26] X. Xue, J. Fang, X. Ai *et al*., "A fully distributed ADP algorithm for real-time economic dispatch of microgrid," *IEEE Transactions on Smart Grid*, doi: 10.1109/TSG.2023.3273418.
[27] M. Dolatabadi, A. Borghetti, and P. Siano, "Scalable distributed optimization combining conic projection and linear programming for energy community scheduling," *Journal of Modern Power Systems and Clean Energy*, vol. 11, no. 6, pp. 1814-1826, Nov. 2023.
[28] X. Kou, F. Li, J. Dong *et al.*, "A scalable and distributed algorithm for managing residential demand response programs using alternating direction method of multipliers (ADMM)," *IEEE Transactions on Smart Grid*, vol. 11, no. 6, pp. 4871-4882, Nov. 2020.
[29] H. Fan, C. Duan, C. K. Zhang *et al.*, "ADMM-based multiperiod optimal power flow considering plug-in electric vehicles charging," *IEEE Transactions on Power Systems*, vol. 33, no. 4, pp. 3886-3897, Jul. 2018.
[30] S. Cui, Y. Wang, and J. Xiao, "Peer-to-peer energy sharing among smart energy buildings by distributed transaction," *IEEE Transactions on Smart Grid*, vol. 10, no. 6, pp. 6491-6501, Nov. 2019.
[31] S. Mao, Z. Dong, P. Schultz *et al.*, "A finite-time distributed optimization algorithm for economic dispatch in smart grids," *IEEE Transactions on Systems*, *Man*, *and Cybernetics*: *Systems*, vol. 51, no. 4, pp. 2068-2079, Apr. 2021.
[32] H. M. Chung, S. Maharjan, Y. Zhang *et al*., "Distributed deep reinforcement learning for intelligent load scheduling in residential smart grids," *IEEE Transactions on Industrial Informatics*, vol. 17, no. 4, pp. 2752-2763, Apr. 2021.
[33] K. Li, X. Ai, J. Fang *et al*., "Coordination of macro base stations for 5G network with user clustering," *Sensors*, vol. 21, no. 16, p. 5501, Aug. 2021.
[34] H. Lin, K. Hou, L. Chen *et al*., "Unit commitment of high-proportion of wind power system considering frequency safety constraints," *Power System Technology,* vol. 45, no. 1, pp. 1-13, Jan. 2021.
[35] M. Zhang, X. Ai, J. Fang *et al*., "A systematic approach for the joint dispatch of energy and reserve incorporating demand response," *Applied Energy*, vol. 230, pp. 1279-1291, Nov. 2018.
[36] X. Xue, J. Fang, X. Ai *et al*., "Real-time joint regulating reserve deployment of electric vehicles and coal-fired generators considering EV battery degradation using scalable approximate dynamic programming," *International Journal of Electrical Power & Energy Systems*, vol. 140, p. 108017, Sept. 2022.
[37] Y. Lin, X. Li, B. Zhai *et al*., "A two-layer frequency control method for large-scale distributed energy storage clusters," *International Journal of Electrical Power & Energy Systems*, vol. 143, p. 108465, Dec. 2022.
[38] *Technical Specification for Connecting Wind Farm to Power System – Part 1: Onshore Wind Power*, GB/T 19963.1-2021.

**Kun Li** received the B.Eng. degree in Wuhan University (WHU), Wuhan, China, in 2020. He is currently pursuing the Ph.D. degree in electrical engineering with the Huazhong University of Science and Technology (HUST), Wuhan, China. His research interests include frequency-constrained operation optimization of power system, ancillary service market, and energy management of 5G base stations.

**Jiakun Fang** received the B.Eng. and Ph.D. degrees from Huazhong University of Science and Technology (HUST), Wuhan, China, in 2007 and 2012, respectively. From 2012 to 2019, he was with the Department of Energy Technology, Aalborg University, Aalborg, Denmark. He is currently a Professor with the School of Electrical and Electronics Engineering, HUST. His research interests include optimization of integrated energy transmission systems for electricity, refined oil and natural gas, power-to-hydrogen and its applications, and partial differential constrained optimization.

**Xiaomeng Ai** received the B.Eng. degree in mathematics and applied mathematics and the Ph.D. degree in electrical engineering from Huazhong University of Science and Technology (HUST), Wuhan, China, in 2008 and 2014, respectively. He is currently an Associate Professor with HUST. His research interests include robust optimization theory in power system, renewable energy integration, and integrated energy market.

**Shichang Cui** received the B.Eng. degree in automation and the Ph.D. degree in control science and engineering from the Huazhong University of Science and Technology (HUST), Wuhan, China, in 2016 and 2021, respectively. From September 2019 to September 2020, he was visiting the Department of Mechanical Engineering, University of Victoria, Victoria, Canada, supported by the China Scholarship Council (CSC) Joint Doctoral Program. He is currently a Postdoctoral Fellow with the State Key Laboratory of Advanced Electromagnetic Engineering and Technology, School of Electrical and Electronic Engineering, HUST. His research interests include stochastic optimization, distributed optimization, game theory, and energy management for smart grids.

**Rongkang Zhao** received the B.Eng. degree in electrical engineering from the Huazhong University of Science and Technology, Wuhan, China, in 2023, where he is currently working toward the Ph.D. degree in electrical engineering. His research interests include power system operation optimization.

**Jinyu Wen** received the B.Eng. and Ph.D. degrees in electrical engineering from Huazhong University of Science and Technology (HUST), Wuhan, China, in 1992 and 1998, respectively. He was a Visiting Student from 1996 to 1997 and Research Fellow from 2002 to 2003 at the University of Liverpool, Liverpool, UK, and a Senior Visiting Researcher at the University of Texas at Arlington, Arlington, USA, in 2010. From 1998 to 2002, he was a Director Engineer with XJ Electric Co., Ltd. China. In 2003, he joined the HUST and now is a Professor with the School of Electrical and Electronics Engineering, HUST. His current research interests include renewable energy integration, energy storage, multi-terminal HVDC, and power system operation and control.